Carbonates and Evaporites (2023) 38:9
https://doi.org/10.1007/s13146-022-00829-7

ORIGINAL ARTICLE

Sedimentology, geochemistry, and geomorphology of a dry-lake playa, NE Iran: implications for paleoenvironment

Maliheh Pourali[1] · Adel Sepehr[2] · Ziba Hosseini[3] · Mohammad Ali Hamzeh[4]

Accepted: 7 November 2022 / Published online: 30 November 2022

Abstract

This study aims to investigate Sabzevar playa in the northeast of the Great Kavir in terms of geomorphology, bulk and clay mineralogy, as well as the geochemistry of core sediments from the surface to a depth of 1 m. The results suggest that up to 50% of Sabzevar playa is made of clastic components (mostly quartz and clay minerals), which increases toward the depth, though this trend is bucked by evaporite minerals (mostly gypsum, calcium carbonate, and halite). According to the mineralogical trend and geochemical evidence, Sabzevar brine has evolved into a Na–SO_4–Cl type. Granulometry studies suggest drastic fluctuations and higher energy costs during sediment deposition at a depth of 1 m compared to the surface. The micro-morphology of quartz grains is due to the windborne surface sediments and waterborne deep grains. A combination of clay mineralogy and geochemistry of elements exhibits a higher evaporation rate at the surface than at a depth of 1 m, suggesting that the area has witnessed a climate change from a warm humid climate in the past to a warm arid climate in recent years. Sabzevar playa is characterized by an unconventional Bull's-eye pattern with a concentration of calcite around the playa, gypsum in the center, and halite in the west. This research also explores the hydrological characteristics of the study area based on geomorphologic surfaces findings revealing that the groundwater level was higher in the west than in the center and east of Sabzevar playa, leading to the formation of halite and the development of a salt pan in the margin.

Keywords Paleoenvironmental reconstruction · Sebzevar playa lake · Sediment · Clay mineralogy · Late Quaternary

Introduction

Playas are closed or very limited basins that constitute one of the ideal systems for paleoclimatic and paleoenvironment research (Abdi et al. 2018; Jalilian et al. 2021; Hardie et al. 1978). They appeared mostly in arid and semi-arid regions in the Late Quaternary (e.g., Sinha et al. 2006; Owen et al. 2007; May et al. 2015; Jalilian et al. 2021). The evaporated mineral assemblages and salt geochemistry change during the brine evolution and the formation of playas (e.g., May et al. 2015; Lukich et al. 2020; Richoz et al. 2017; Abdi et al. 2018; Pourali et al. 2020). Their mineralogy and geochemistry are determined by the balance between a host of factors such as evaporation, participation, rainfall, water charges, clay mineral conversions, and sulfate reduction rate (Rosen 1994; Yan et al. 2002; Jones and Deocampo 2003; Roy et al. 2008; Erfanian Kaseb et al. 2020). These characteristics highlighted the importance of the playa for researchers working on paleo-depositional and paleoclimate research in recent years (Rosen 1994; Sinha et al. 2006; Hminna et al. 2020; Schroder et al. 2018; Han et al. 2019; Zhang et al. 2022; Xia et al. 2022). Acting as a sink for dust in some cases, playas can be hydrologically important as they influence the groundwater quality in their surrounding areas (Yechieli and Wood 2002; Hahnenberger and Nicoll 2014) considering their geochemistry and interaction with water (Hosseini et al. 2016).

✉ Maliheh Pourali
maliheh.pourali@mail.um.ac.ir

✉ Adel Sepehr
adelsepehr@um.ac.ir

[1] Department of Geography, Faculty of Letters and Humanities, Ferdowsi University of Mashhad, Mashhad, Iran

[2] Department of Desert and Arid Zones Management, Faculty of Natural Resources and Environment, Ferdowsi University of Mashhad, Mashhad, Iran

[3] Department of Geology, Faculty of Science, Ferdowsi University of Mashhad, Mashhad, Iran

[4] Iranian National Institute for Oceanography and Atmospheric Science (INIOAS), Tehran, Iran

Iran has been under compressional tectonic events since 65 Ma, squeezed between the Arabia and Eurasia plates, and is distinguished by pronounced rigidity (Berberian 1981). This tectonic setting has given rise to several orogenic belts with intermountain basins. A dramatic change in the Late Quaternary climate contributed to the development of more than 60 playas in Iran (Krinsley 1970; Vaezi et al. 2019). Several studies have focused on Iran's playas, exploring various topics such as geomorphology, hydrogeology, sedimentology, and environmental effects. Accordingly, topics such as brine evolution and formation of the Saghand playa (Torshizian 2009), the paleoclimate of Meyghan playa (Abdi et al. 2018), Jazmourian playa (Vaezi et al. 2019), and Gavkhouni playa (Jalilian et al. 2021), the transportation mechanism associated with the sequences of Jazmourian playa (Zandifar et al. 2022), the hydrochemistry of Shahrokht-Yazdan playa brines (Erfanian Kaseb et al. 2020), and the tectonic geomorphology of Ernan playa (Sharifi Paichoon 2021) have been explored. Most of these studies have looked into playas in southern Iran, where Lut and Jazmurian deserts are located, and in central Iran, which is home to Great Kavir (GK) (Fig. 1a). Few studies have investigated the geomorphologic characteristics of playas in northeastern Iran (e.g., Ghasemzadeh Ganjehie et al. 2018; Pourali et al. 2020).

The present research is conducted on the Sabzevar playa in the northeast of the Great Kavir (Fig. 1b). Sabzevar playa had been identified and demarcated by Krinsley (1970), and there is no more comprehensive study after it. Knowledge of formation mechanisms is needed for this playa which certainly provides information on the rate of climate changes and underground water circulation systems and can be applied in analyzing whether the current situation of the playa has an association with future developments. So, a general model is presented to describe how the Sabzevar playa is formed. The study suggests how mineralogical and geochemical characteristics distinguish wet periods from dry spells during the Late Quaternary. Moreover, evaporite and clay minerals are discussed on their diversity, origin, and distribution. This study helps shed light on the transport mechanisms of playa sequences by interpreting brine evolution based on mineralogical trends and provides some information on the paleohydrology of the Sabzevar playa.

Study area and geological setting

The Sabzevar playa, stretching in an area of approximately 120 km, is one of the most elongated depressions in Khorasan Razavi province in northeastern Iran covering an area of 2648 km^2 and located between 35°55′–36°25′ north latitude and 56°15′–57°45′ east longitude. The Sabzevar playa is often classified along with Great Kavir and its surrounding playas (e.g., Damghan Kavir, Bajestan playa, Haj Aligholi Kavir) under the name of the "Dasht-e Kavir" basin (Fig. 1a) (Jouladeh Roudbar et al. 2015). The playa has an arid and hot climate with a mean annual temperature of 17.50 °C and an average annual rainfall of about 150–200 mm (based on reports of Sabzevar synoptic station considered the period between the years 1955 and 2010). Topographically, Sabzevar playa is classified as a flat area and its main river "Kal-Shour" is ephemeral (Fig. 1b). the headwaters of the river, originating from Binalud Mountain, flow west in the playa where they meet the south-flowing Kal-e Khartouran River (Pourali 2020). The topographic elevation, varying between 750 and 900 m above sea level (m a.s.l), is on average over 800 m a.s.l. It tends to be higher in the east with a general downslope to the west along the Kal-Shour river. Although nowadays, Sabzevar playa has seasonal hydrological currents, according to Krinsley (1970), it was a closed basin during the Pliocene. In fact, after Pliocene, Sabzevar playa converted to a semi-closed basin due to the influence of fault activity. The regional geomorphology consists of three dominant geomorphic surfaces, including clay pan, puffy ground and salt crust. (e.g., Neal 1972; Smoot and Lowenstein 1991; Czarnecki 1997; Argaman et al. 2006; Abdi et al. 2018). A clay pan is a surface covered by dry fine-grained sediments that are strongly compacted and hardened, and normally do not exhibit traces of dust emission. The puffy ground is a friable surface characterized by crust expansion. This geomorphologic characteristic is created by evaporation where the groundwater level is low. The salt pan of Sabzevar playa is characterized by two common features, polygonal crusts and spongy efflorescent popcorns that developed due to high concentrations of halites. The geological nature of the playa includes alluvial and evaporation sediments belonging to the Quaternary period. Windborne sand dunes, tertiary igneous rocks, and Cretaceous carbonates (dolomite and limestone) are mainly found in the neighboring mountain flanks (Geological Survey of Iran 2005), as shown in Supplementary Fig. 1 (Online Resource 1). Some areas in the periphery of Sabzevar playa also contain ophiolite sequences called Sabzevar ophiolites. Intrusive and volcanic units are mainly found around the northern and eastern parts of the playa. Furthermore, carbonates and detrital sedimentary units containing conglomerates and sandstone are scattered with abundant outcrops.

Materials and methods

Sampling

From July to August 2018, 80 sediment samples were collected using a hand auger manufactured by the German company Windas, from profiles that were 5 cm in diameter and

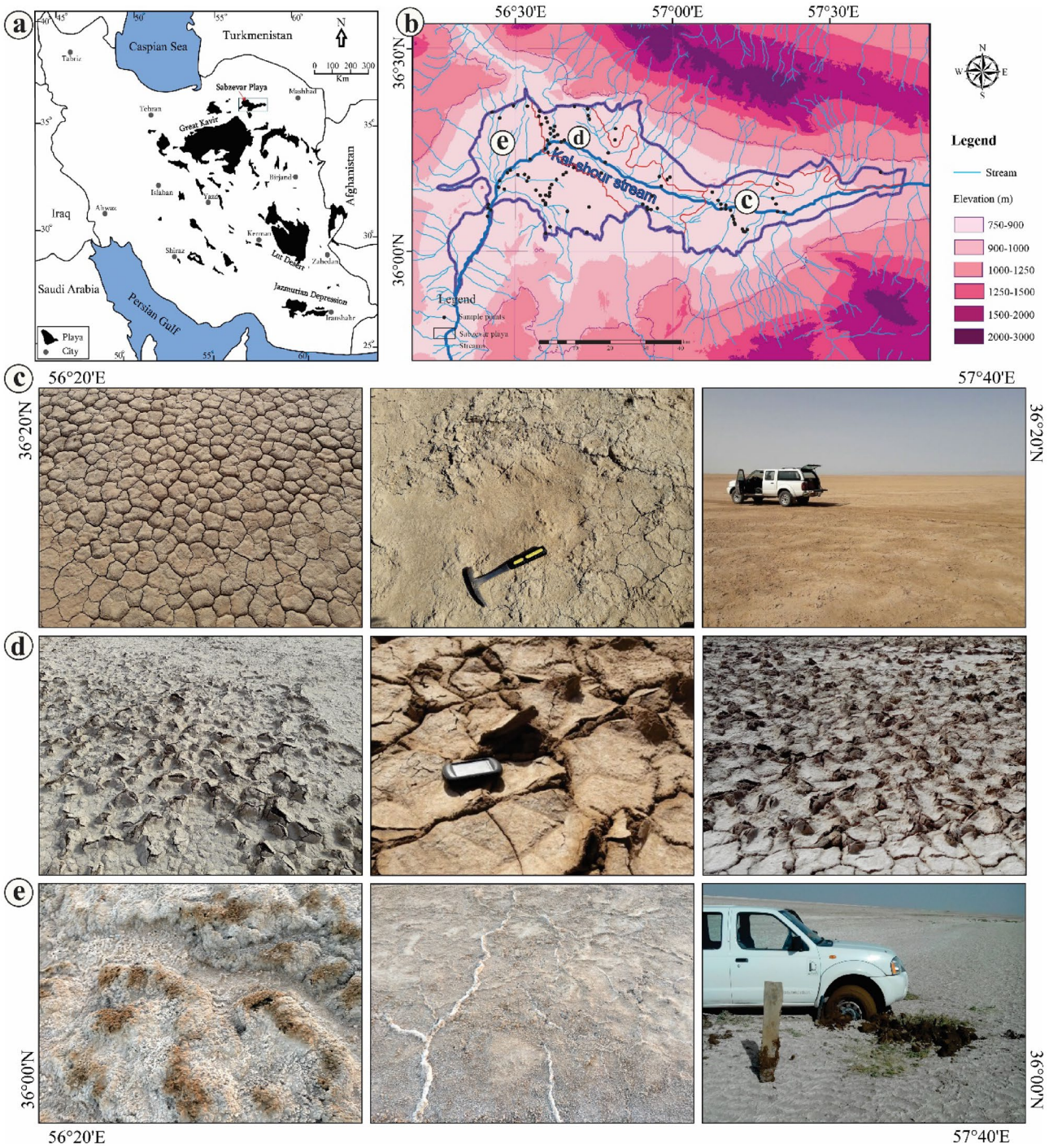

Fig. 1 **a**, **b** Location of Sabzevar playa in Iran (Krinsley 1970) and its topographical or hydrological characteristics in relation to the geomorphic surface together with the sampling points, **c** clay pan **d** puffy ground **e** salt crust

100 cm in depth perpendicular to the surface of the playa. They were gathered from three geomorphic surfaces, including a clay pan, puffy ground, and a salt crust that represents changes under study. The general position of the three main geomorphological surfaces and the position of profiles are shown in (Fig. 1b–e).

Locations were recorded by a handheld Global Positioning System (GPS), and profiles were drawn from the surface up to a maximum depth of 1 m. Four depth intervals (0–10 cm, 30–40 cm, 60–70 cm, 90–100 cm) of each profile were selected in terms of variations in color, texture,

and grain sizes of sediments, As given in Supplementary Fig. 2 (Online Resource 1).

Laboratory analyses

Air-dried sediment samples were passed through a 2-mm sieve prior to analyses. The pH values were determined in a suspension with a sediment-to-water ratio of 1: 2.5 using a pH meter (Jenway Inc, England). The electrical conductivity (EC) was measured in a suspension with a sediment-to-water ratio of 1:5 at 25 °C by an EC meter (Jenway Inc, England) (Rayment and Lyons 2011). Organic matter (OM) content was also measured by the modified Walkley–Black procedure proposed by Nelson and Sommers (1996) at the laboratory of Ferdowsi University's Natural Resources and Environment Faculty.

One hundred and sixty air-dried powder samples from 4 studied depths (0–10 cm, 40–60 cm, 60–70 cm, 90–100 cm) were examined to identify both bulk and clay mineralogy using the X-ray diffraction (XRD) (Philips PW1730, Germany) (Bruker_ D8 ADVANCE, Germany) at the central laboratory of the Ferdowsi University of Mashhad and Razi Applied Science Foundation in Tehran. The clay-sized minerals were prepared based on Jackson's treatment (Jackson 2005) and analyzed by XRD three times: on air-dry slides, after ethylene–glycol treatment, and after heating at 550 °C. The XRD diffractograms were interpreted using the HighScore (Plus) program and Match3.

The concentration of elements was estimated using ICP-MS (Van de Wiel 2003). About 500 mg of powdered sediment was decomposed with a mixture of concentrated nitric acid, hydrochloric acid, and hydrofluoric acid. The concentration of elements in the sample solution was determined in triplicate using optical emission spectroscopy with inductively coupled plasma (SpectroArcos-76004555 plasma, Germany) at the central laboratory of the Ferdowsi University of Mashhad. The major concentrations of oxide and trace elements were determined by X-ray fluorescence (XRF) (Philips PW1410/70) based on ppm and according to the procedure explained by Abdi et al. (2018). As major representatives of environmental changes (wet/dry periods), the elemental ratios of TiO_2/Al_2O_3, SiO_2/Al_2O_3, K_2O/Al_2O_3, Na_2O/TiO_2, Zr/Al_2O_3, Na_2O/K_2O, Na/Fe, Na/Ti/, Na/Al, Sr/Ba and Rb/Sr were calculated at surface and depth.

Scanning electron microscopy (SEM) (VP 1450, LEO—Germany) and energy dispersive X-ray (EDX) analysis were conducted for 20 samples to identify the bulk and clay minerals, determine the morphology of quartz grains, and evaluate their relationship with the selected depth intervals at the central laboratory of the Ferdowsi University of Mashhad. The Geographical Information Systems (GIS) were also exploited to map and analyze the geomorphologic features of the study area. To investigate the shape of quartz grains, pre-treatment procedures described by Vos et al. (2014) were used. They explained steps to chemically remove other components such as carbonates, organic matter, and iron oxides. SEM analysis was also conducted using the method described by Itamiya et al. (2019). The grain size classification was based on Folk and Ward (1957). A laser particle size analyzer (Horiba Partica LA-950) was utilized to determine grain sizes (Ashley 1978) at the Iranian National Institute for Oceanography and Atmospheric Science Laboratory of Tehran. The phrase "surface and depth samples" in this paper describes samples derived from a depth of 0–10 cm and 90–100 cm of each profile, respectively. The data obtained from laser particle size analysis conducted by the GRADISTAT software version 9/1 (2020) was used to analyze the grain-size distribution and calculate its parameters such as sorting, skewness and kurtosis (Blott and Pye 2001) for each profile (0–10 cm, 90–100 cm depths). The mean grain size (Mz), standard deviation (δI), skewness (SKI), and kurtosis (K) were calculated using the following equations (Eqs. 1–4), (Folk and Ward 1957):

$$MZ = \frac{\varnothing 16 + \varnothing 50 + \varnothing 84}{3} \tag{1}$$

$$\delta I = \frac{\varnothing 84 - \varnothing 16}{4} + \frac{\varnothing 95 - \varnothing}{6.6} \tag{2}$$

$$SKI = \frac{\varnothing 16 + \varnothing 84 - 2\varnothing 50}{2(\varnothing 84 - \varnothing 16)} + \frac{\varnothing 5 + \varnothing 95 + 2\varnothing 50}{2(\varnothing 95 - \varnothing 5)} \tag{3}$$

$$K = \frac{\varnothing 95 - \varnothing 5}{2.44(\varnothing 75 - \varnothing 25)} \tag{4}$$

Results

Sedimentology

The Sabzevar playa sediments chiefly include evaporite minerals in the western and clastic minerals in the eastern part of the area. We identified three main surfaces in the Sabzevar playa stretching from the east to the west of the playa. They display a wide range of geomorphologic surfaces classified as clay pan, puffy ground, and salt crust. Surface sediments comprise sand and silt dominated in the east, which are converted to silty-clayey grain sizes in the west (Fig. 2). Samples taken from the surface up to a depth of 1 m exhibit about 10% surge in silt size particles as well as the reduction in the sand grains, as can be seen in Supplementary Table 1 (Online Resource 1).

Generally, Sabzevar sediments have a silty to sandy-silt texture. Although the mean particle size is 6 ϕ in the

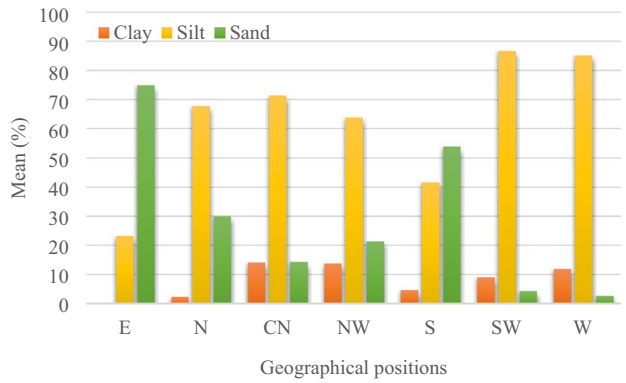

Fig. 2 Mean grain size distribution in the different geographical positions of Sabzevar playa

profiles, sediments lack any identical granulometry features. Surface to deep samples tends to be poorly sorted, indicating higher values for sorting parameters at a depth of 1 m. Skewness is characterized by an asymmetric to roughly symmetrical distribution with both positive and negative values. The kurtosis values ranged from 0.7 to 1.3 for upper samples (0–10 cm), which are almost platykurtic to leptokurtic. The kurtosis manifested an increasing trend toward deeper locations (90–100 cm), yielding values of 1–1.6, which had a mesokurtic to a very leptokurtic pattern (Fig. 3).

Physical and chemical analysis

The mean organic matter (OM) was approximately 0.6% and comparable in surface and deep samples derived from the east. Also, the pH values in the range of 7.08 to a maximum of 9.3 suggested a slightly alkaline to alkaline nature. The mean pH was 8.5 in the upper samples, dropping mildly to 8.1 in the deeper samples. Recorded ECs were in the range of 0.21–59 with all profiles exposing a reduction in deeper layers, as shown in Supplementary Table 1 (Online Resource 1).

Mineralogy

Bulk XRD showed clastic, evaporite, and carbonate minerals, As given in Supplementary Table 1 (Online Resource 2). **Clastic minerals**, accounting for up to 50% of the mass, are frequently identified as quartz and clay-sized minerals with the lesser feldspar. Quartz is the most dominant clastic mineral with a monocrystalline appearance, which was derived from non-deformed igneous rocks in the catchment basin (Pourali 2020). The quartz crystals have a distinctive and variable morphology at the surface compared to samples at a deep of 1 m. Samples derived from the top 10 cm had an angular and sub-angular grain with sharp linear fractures, high relief, and curved grooves, showing broken edges and conchoidal breakages on edges whereas those collected from a depth of 1 m were more subangular with V-shaped percussion, medium relief, visible traces of chemical weathering and abraded fractures (Fig. 4); however, a small number of grains corresponded to the superficial grains.

Clay minerals represent a variety of minerals appearing in three main assemblages based on their frequency in Sabzevar playa, including:

1. Kaolinite, illite, smectite, chlorite,
2. Palygorskite, sepiolite, smectite, and
3. Smectite, vermiculite, kaolinite, chlorite.

The ratio of clay minerals in each assemblage varies, but clay minerals tend to increase towards depth, reaching their

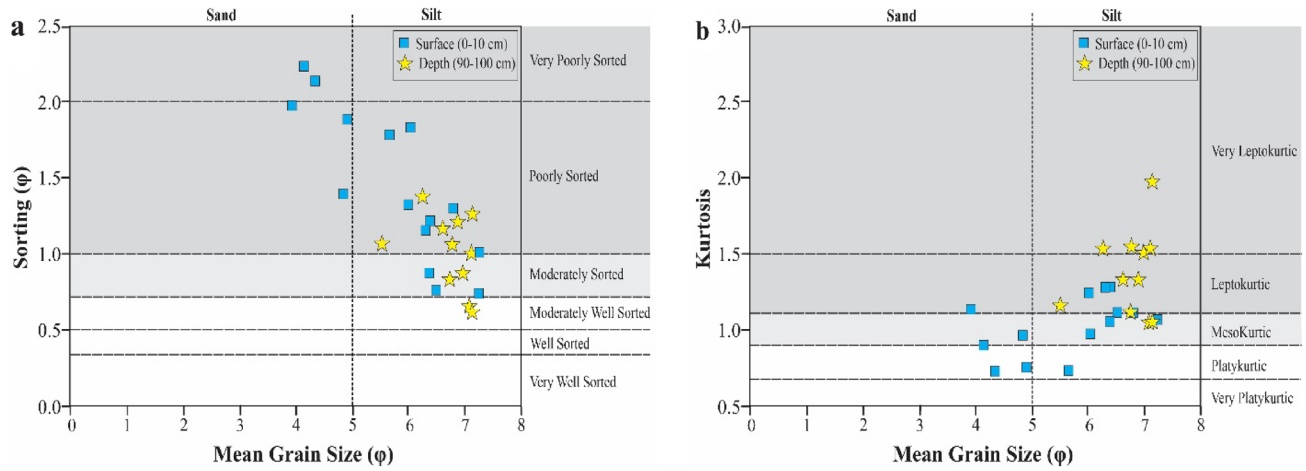

Fig. 3 Correlation between textural parameters of sediments. **a** Sorting vs. mean grain size showing poor sorting for surface sediments, **b** kurtosis vs. mean grain size reflecting depth sediments' tendency to be more leptokurtic than surface

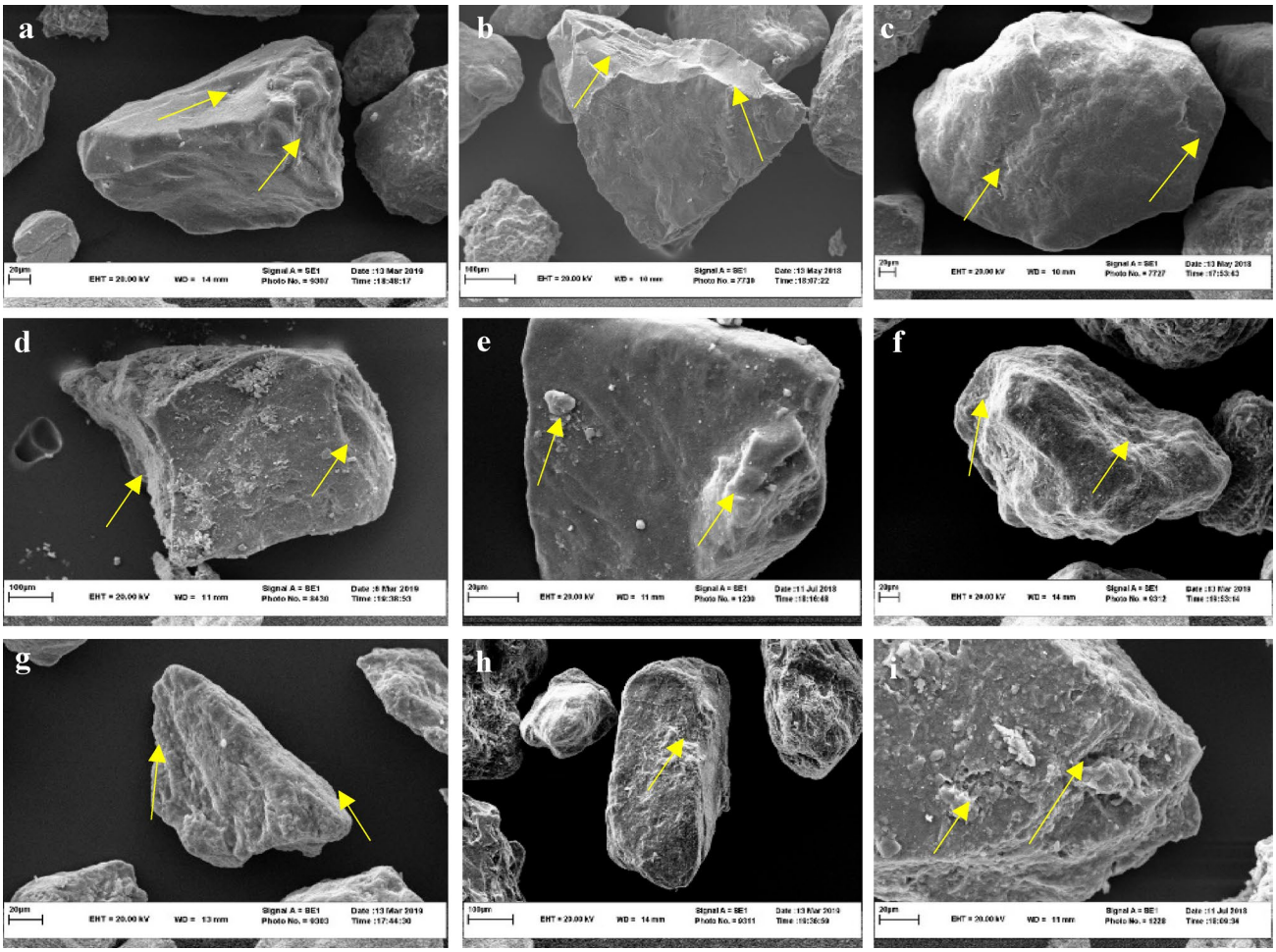

Fig. 4 Quartz grains' surface microtextures at various depths or places of the Sabzevar playa were detected using SEM. Every picture of the examples above has evident aeolian or fluvial characteristics: **a** Aeolian quartz grain with subangular fractured edges (0–10 cm depth, center playa), **b** the grain of aeolian quartz is triangular and has conchoidal breakages on the edges (0–10 cm depth, south playa), **c** aeolian quartz grain with rounded edges, smooth surfaces, and evidence of pitting both large and little (0–10 cm depth, south playa), **d** and **e** fluvial quartz grains having large depressions in the form of dishes and V-shaped grooves, with clay-sized particles stuck to these characteristics (60–70 cm depth, northwest playa and 90–100 cm depth, northwest playa), **f** fluvial quartz has a surface that is micro-pitted and shows signs of chemical weathering (60–70 cm depth, center playa), **g** aeolian quartz is composed of sub-angular quartz grains with broken edges and morphological characteristics indicative of eolian transport (30–40 cm depth, center playa), **h** fluvial quartz showing prolate grains which reflect etching and weathering (90–100 cm depth, north playa), **i** a fluvial quartz grain with subangular, bulbous edges that exhibit high relief and adherent particles (60–70 cm depth, north playa)

peak between 60 and 70 cm depths. Clay minerals can be detrital or formed by the chemical weathering of feldspars (authigenic). The study area was not suited for the authigenic formation of the first assemblage including kaolinite, illite, and chlorite, because, as reported in several arid to semi-arid environments in Iran, these clay minerals were detrital (e.g., Khormali and Abtahi 2003; Owliaie et al. 2006; Farpoor et al. 2012). As indicated by the intensity ratio of peak 002/003 illite (Środoń 1984), the mixed-layer illite–smectite containing 30–50% smectite is exhibited in Supplementary Fig. 3 (Online Resource 1). It suggests that a part of smectites was detrital because authigenic interstratified illite–smectite typically reflects less than 30% of illite (Środoń 1984). The second assemblage was chiefly concentrated on parts with evaporite minerals, and SEM revealed that clays in this assemblage were fibrous in shape (Fig. 5). Clays in the high pH area had fine-textured sediments and scattered to the east and west of the playa. Under such environments, as reported in the literature, sepiolite and a small number of smectites displayed authigenic formation, (Farpoor et al. 2002; Owliaie et al. 2006; Farpoor et al. 2012). Palygorskite was observed at a depth higher than 60 cm with smectite that exhibits a genetic relationship between them and somehow the transformation of smectite

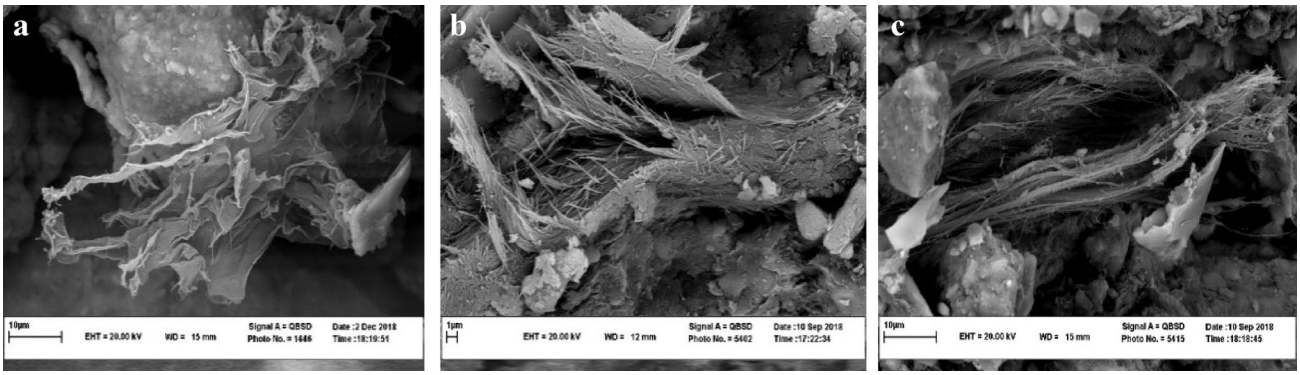

Fig. 5 Scanning electron microscopy (SEM) images of clay minerals from different depths or positions of the Sabzevar playa: **a** smectite texture (60–70 cm depth, Southwest playa), **b** images of the growth of sepiolite fibers (90–100 cm depth, west playa), **c** palygorskite fibers (90–100 cm depth, Southwest playa)

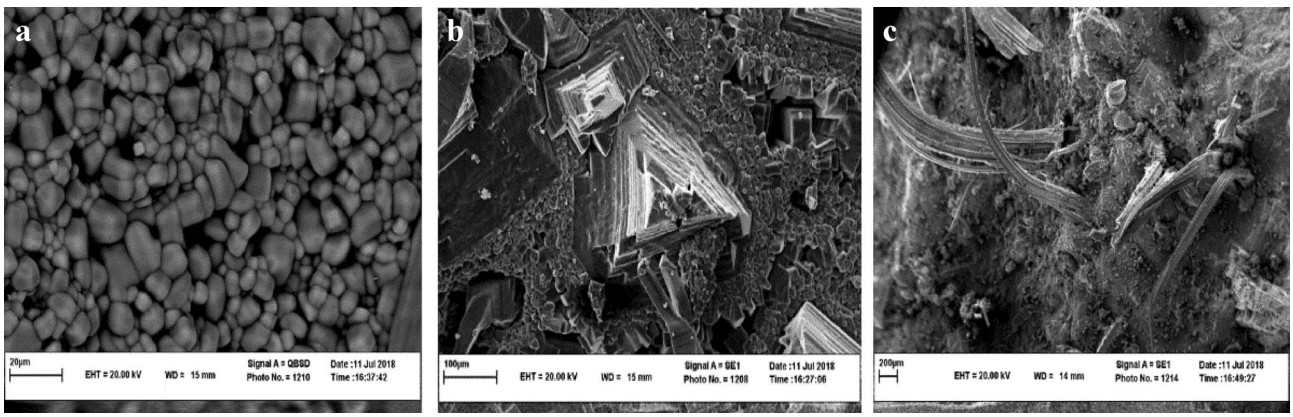

Fig. 6 Scanning electron microscopy (SEM) of different shapes of halite mineral crystals from different depths or positions of the Sabzevar playa **a** cubes of halite (0–10 cm depth, west playa), **b** Halit in the shape of triangular pyramids (30–40 cm depth, west playa), **c** halite needle-shaped form (0–10 cm depth, west playa)

to palygorskite (cfr. Xie et al. 2013). The third assemblage with a lower frequency mostly contains clastic sediments and all clay minerals in this assemblage have probably originated inherited. The maximum frequency of this assemblage was documented in depths of 60 and 70 cm, while the first assemblage of clay had a higher frequency on the surface. The third assemblage, The XRD peak, reflects analcime as the main type of zeolite in the study area. Analcime was observed with albite in the margin of the playa where pH is above 9. The corrosion of albites proves the impact of chemical weathering (Pourali 2020).

Among **evaporite minerals**, sulfates and chlorides take up 30%. They include gypsum ($CaSO_4•2H_2O$), polyhalite ($K_2Ca_2Mg(SO_4)_4•2H_2O$), anhydrite ($CaSO_4$), halite (NaCl), glauberite ($Na_2Ca(SO_4)_2$), and very small amounts of sylvite (KCL). Gypsum and halite are the most prevalent sulfate and chloride minerals, respectively. Gypsum is more abundantly found in the center of the playa and deep layers as opposed to halite, which is chiefly found to the south and west of the Sabzevar playa, where gypsum, clastic, and carbonates minerals have a lower quantity as opposed to the center and the east. The distribution of polyhalite and glauberite resembles that of halite. It is worth noting that the thickness of pure halite layers barely exceeds a few Centimeters in the playa. In our samples, halite morphology was in the form of pyramidal hoppers and subhedral fine cubes. Subhedral cubes of halite are filled by pores between pyramidal hoppers in the air-brine interface. Moreover, fibrous-shaped halites and clay-sized minerals are observed in salt crusts in the west of the playa (Fig. 6).

Carbonate minerals originating from chemical and clastic processes make up approximately 20% of surface and deep sediments. Carbonates have accumulated across the playa but their distribution is more pronounced in the east than in the west. Calcite ($CaCO_3$) is more profusely found in this class, but dolomite ($CaMg(CO_3)_2$), ankerite ($Ca(CO_3)_2$),

huntite ($Mg_3Ca(CO_3)_4$), and natron (NA_2CO_3•$10H_2O$) are also found in this category. High Mg-calcite and low Mg-calcite are differentiated based on unit cell parameters provided by XRD analysis. High Mg-calcite represents the highest reflection on 29.8–29.9 2θ and d104 ≈ 2.98 Å and is commonly observed in low amounts with dolomite. Low Mg-calcite indicates the main peak of 29.4° 2θ equivalent to d104 ≈ 3.03. It is found with dolomites where quartz is formed. The XRD results also suggested that dolomites are observed in stoichiometric crystal structures. They are almost pure dolomites with an intensity peak of 104 on 31° 2θ. The pure dolomites are primarily accumulated in a deep interval with low Mg-calcite. Huntite and ankerite are not associated with the distribution of Mg-calcites, and natron is barely found.

Geochemistry of elements

XRF analysis showed that SiO_2 makes up an average of 43% in the upper samples and 39% in the deep samples, as displayed in Supplementary Table 1 (Online Resource 3). Playa is a place for sediment accumulation where abundant SiO_2 is found in the form of silicate sediments (wind-blown and alluvial) on the surface of the playa. Identified as the most profuse oxide in the Sabzevar playa, it is combined with MgO, Al_2O_3, and CaO, accounting for 7 to 9% of superficial and deep samples. There is a positive correlation between SiO_2 and Al_2O_3, K_2O, TiO_2, and Fe_2O_3 suggesting that the high content of SiO_2 is derived from quartz, feldspar, and clay minerals. SiO_2 was negatively correlated with the Na_2O content. Sr enrichment is associated with the appearance of calcite and gypsum and the growth of CaO. However, MgO mirrors an increase in horizons with dolomite and palygorskite where CaO content may fall due to the absence of calcite. Large amounts of Fe, Mg, Cu, Rb, Co, and Ba-bearing sediments are generally deposited in humid climate whereas sediments deposited in arid climate conditions mainly contain Sr, Na, Ca, Mg, and Zn (Stankevica et al. 2020). According to this, various proxies have evolved to reconstruct the paleoclimate. The highly soluble cations like Na^+ and Mg^{2+} behave differently than insoluble cations such as Ti^{4+}, Al^{3+}, and Fe^{3+} (Mason and Moore 1982), which are resistant to normal weathering solutions. Due to its relatively larger ionic radius and partial immobility, the behavior of the soluble cation K^+ is distinctive. It dissolves (like Na^+) but is also adsorbed quickly, forming new compounds (e.g., illite) (Pandarinath et al. 1999). However, the ratios Na/Ti, Na/Al, and Na/Fe, strongly increase with aridity. Moreover, arid periods are known by high dust inputs and typically have high SiO_2/Al_2O_3 and TiO_2/Al_2O_3 ratios (Martinez-Ruiz et al. 2015).

On the other hand, a high Rb/Sr ratio is generally observed in humid climates, in which Sr is lost due to high precipitation while Rb is relatively stable (Du et al. 2011; Chang et al. 2013). A Higher K_2O/Al_2O_3 ratio is also indicative of higher alluvial inputs (Martinez-Ruiz et al., 2015). On this basis, we compared the variation of these climate-sensitive elements at the surface and at a depth of 90–100 cm to explore climate changes in the area. Surficial enrichment of Na_2O/TiO_2 and Na_2O/K_2O indicates more arid conditions in recent years. In addition, a decrease in TiO_2/Al_2O_3 and SiO_2/Al_2O_3 from the surface to the depth (especially in the west) is attributed to greater aeolian flux from the past to the present. During the past wetter period, it is likely that the playa has been subject to greater chemical weathering (Fig. 7); a higher K_2O/Al_2O_3 ratio suggests higher alluvial inputs in the past. The dissolved Sr^{2+} entering the playa is generally deposited with the carbonates in the dry period, thus increasing the Rb/Sr ratio in the past wetter environment. The ratio of Zr/Al_2O_3, which rises in the deeper layers, is positively correlated with the quantity of SiO_2/Al_2O_3. The opposite is true for ratios of Sr/Ba, which are positively correlated with the content of CaO. Metals such as Zn, Pb, Cu, and Rb are positively correlated with Sr/Ba and CaO but negatively related to SiO_2 and Zr. Rb decreases gradually with depth, demonstrating an opposite trend with Zr. It is noteworthy that there is a direct relationship between P_2O_5 and Fe_2O_3 supporting the abiotic origin of phosphorus (cfr. Roy et al. 2006).

Discussion

Brine evolution

The type and distribution of mineralogy in a playa are directly dependent on the chemical composition of inflows in the primary lake (Rahimpour-Bonab and Abdi 2012). The input water in a non-marine basin can originate from various sources such as meteoric, hydrothermal, diagenetic, volcanogenic, or other sources. The first stage of mineral deposition in confined basins is usually identical. Brine evolution begins with calcite and continues with gypsum as the main carbonate and sulfate minerals, respectively. In the Sabzevar playa, high Mg-calcite, Ca-dolomites, and palygorskite are detected along with gypsum. This is due to changes in the ratio of Mg:Ca after gypsum participation. Since calcite develops in intervals near gypsum, most carbonate minerals are formed by geochemical processes in the Sabzevar playa. However, traces of calcite and pure dolomite are found in quartz. Stoichiometric dolomite is extremely rare in the Holocene or modern sediments even if brines are oversaturated with CaMg $(CO_3)_2$ (Solotchina et al. 2012). Thus, pure dolomite and low content of calcite content in the Sabzevar playa are probably detrital, originating from the surrounding dolomitized limestone belonging to the Cretaceous age. Glauberite and anhydrite formed after gypsum

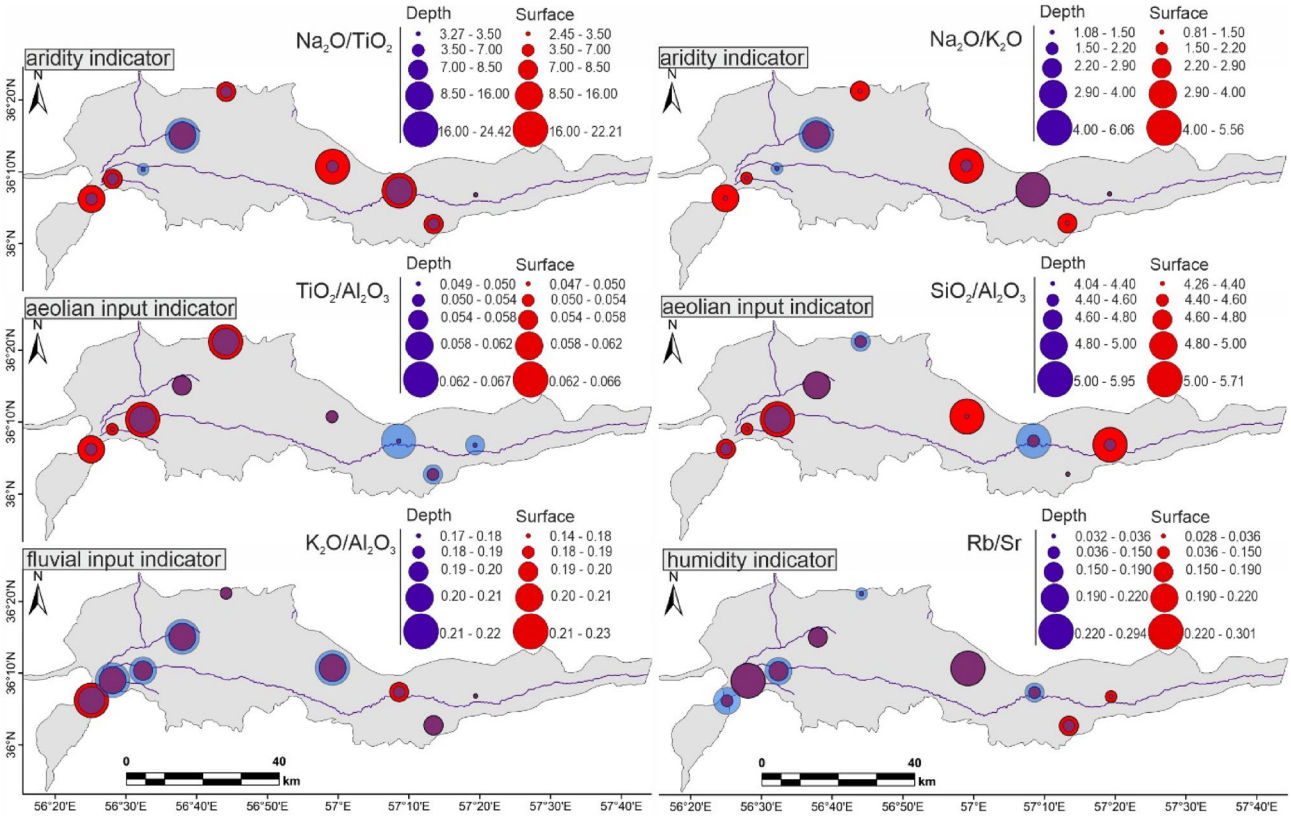

Fig. 7 Variation of selected elemental ratios indicating aridity/humidity in surface (0–10 cm) and depth (90–100 cm) of Sabzevar playa

indicate a high concentration of Ca^{2+} in the brine. Thenardite and mirabilite were not found in our samples. However, their absence in the Sabzevar playa cannot be explained only by high solubility of sodium sulfates. Indeed, since polyhalite pursues the formation of glauberite, the lack of sodium sulfates is probably related to reduced Na^{+} ions compared to other ions such as Ca^{2+}, Mg^{2+}, and K^{+} Polyhalite can be an outcome of relative enrichment of K^{+} and Mg^{2+} in the brine as well as a chemical reaction with primarily deposited sulfates such as anhydrite or glauberite (Shang and Last 1999). When Na^{+} increases in the brine, there will be a small amount of natron with halite. Natron, scarce in the Sabzevar playa, is chiefly found in the Na–CO_3–Cl brine type (Warren 2006). The presence of halite in surface samples indicates higher aridity during a period. However, the halite concentration is higher in the west playa. Sylvite has also been found in a few surface samples. It reflects the depletion of Mg^{2+} in the brine because the high content of Mg^{2+} in the brine often leads to the formation of carnallite rather than sylvite (Ingebritsen and Sanford 1998). According to Panahi et al. (2021), groundwater chemistry in the Sabzevar basin is characterized by a Na–SO_4–Cl type of brine. The mean total dissolved solids (TDS) is higher above 4150 mg/L reaching a maximum of 7600 in the salt flat. TDS forges a strong positive correlation with anions such as Cl^{-}, SO_4^{2-}, HCO^{3-}, and cations Na^{+}, Mg^{2+}, Ca^{2+}, and K^{+}. The ratio of HCO_3/Ca + Mg in the groundwater is on average 1.3 indicating that HCO_3 is lower than Ca + Mg (Panahi et al. 2021). This ratio is heavily reliant on the intensity of bedrock lithology, which plays a vital role in the final composition of brines (Hardie et al. 1978; Roy et al. 2008; Rahimpour-Bonab and Abdi 2012). The lowest ratio of HCO_3/Ca + Mg is found in bedrocks of calcareous sandstones, limestones, and gypsiferous marls in the Sabzevar basin, while the highest ratios are observed in sandstones and diabase bedrocks, as also reported by Panahi et al. (2021). Informed by their minerals and formula, and based on the geochemistry of groundwater in the area, the Sabzevar brine follows path IIB in the diagram of Eugster and Hardie (1978). This pathway suggests the evolvement of brine in a Na-SO_4–Cl type, as shown in supplementary Fig. 4 (Online Resource 1). The playas and saline lakes mostly represent a bull's eye pattern where carbonates occur at the playa's margin while evaporite minerals appear at the center (Tucker 2001). This is the mineralogical distribution of the Sabzevar playa, though halite is concentrated in the west and gypsum in the center of the playa, creating an unconventional distribution in the bull's eye pattern. As mentioned earlier, Sabzevar playa is characterized

by a general downslope with groundwater flowing from the east to the west (Pourali 2020; Panahi et al. 2021). Thus, the distribution of halite has been influenced by the hydrology and topography of the study area. The distribution of halite could be controlled by the hydrology and topography of the study area, as explained in the "Geological setting" section.

The pyramidal hoppers indicate the slow deposition of halite from a supersaturated brine (Pettit and Fontana 2019), where a subhedral cubic cement can be augmented as a result of evaporation, producing fibrous-shaped halite when the brine is drying. The fibrous-shaped halite indicates a solution circulation in the capillary spaces surrounding the older mineralization (Gustavson et al. 1994; Ercan et al. 2019).

Sedimentology and paleoenvironment

Granulometry results and the observed profiles suggest surface-to-deep samples are usually well sorted with an increasing trend for clastic minerals. It exhibits a tendency for deposition at a depth of 1 m in an environment characterized by higher energy than on the surface. However, the depth sediments of western playa are characterized with by poor sorting, which is related to lower energy in the west than in the east playa. In natural environments, high kurtosis values often reflect more drastic fluctuations during sediment deposition (Mir and Jeelani 2015), which is consistent with higher energy conditions at a depth of 1 m. Negative skewness is fairly uncommon in a playa with clay/silt sediments, but it may appear where evaporite minerals with low solubility are concentrated (Abdi et al. 2018). This reveals the dominance of negative values on the west surface of the Sabzevar playa where the salt pan is located and evaporite minerals are largely deposited, as given in Supplementary Table 1 (Online Resource 1).

The surface textural analysis of quartz particles can be used to identify and discriminate the depositional environment (Li et al. 2021). Quartz particles derived from the depth indicate water influx into the basin. The particles are subangular with a medium relief, exhibiting V-shaped percussion and abraded fractures at their surface, which are all attributed to water transportation (Li et al. 2021). However, sediments taken up from the surface had microtextured features induced by wind. Wind transportation generally causes angular grains with sharp linear fractures and high relief (Li et al. 2021). In this regard, although there is no permanent river in the Sabzevar basin, sediments in depth had been deposited under rainfall and floods, suggesting the possibility of permanent rivers flowing in the past, which is in agreement with poor sorting in the depth of the east playa. Clay mineralogy analysis provides information on the aridity and humidity of the climate (Ruffell et al. 2002). Kaolinite is generally accumulated where the degree of leaching is fairly high. It is a residual weathering product in warm humid climates (Pardo et al. 1999) while illite is attributed to cold humid, or cold arid climates (Deconinck et al. 2005), whereas smectite is frequently associated with alternating humid and arid seasons in warm climates (Pardo et al. 1999). The augmented detrital clay minerals (assemblage 1) with the greatest abundance of Kaolinite in the depth display a high degree of humidity and chemical weathering in the past as well as a warm and humid climate. Authigenic clay minerals (palygorskite and sepiolite), mostly formed at the surface, were associated with evaporite minerals. They indicate a period of aridity under a warm climate, which provided suitable geochemical conditions for depositions. The geochemistry of elements also offers evidence for reconstructing paleoclimate (Roy et al. 2006). A high degree of chemical weathering is observed in a humid climate. The ratios of Na_2O/Al_2O_3 and Na_2O/TiO_2 illustrate the transition of soluble oxides to hydrolysates, which can be used to interpret the rate of chemical weathering. The Na_2O/K_2O ratio also displays a similar behavior since potassium is absorbed largely by fine materials. SiO_2/Al_2O_3 and Zr/Al_2O_3 show the degree of terrigenous input in the sediments. At a depth of 1 m, low values of Na_2O/Al_2O_3, Na_2O/TiO_2, and Na_2O/K_2O and high values of SiO_2/Al_2O_3 and Zr/Al_2O_3 are found. These ratios reflect higher humidity in the past, which is aligned with data obtained from clay mineralogy. Humidity provoked clastic inputs into the playa (Smykatz-Kloss and Roy 2010), the intensity of which was increased by depth. A surge in Sr/Ba ratio reflects the prevalence of aridity (Roy et al. 2006). This ratio increases toward the surface, demonstrating that the humidity in Sabzevar playa is lower today than in the past. The higher SiO_2 content exhibits a greater aeolian activity in its surroundings. (Martinez-Ruiz et al. 2015). The wind has transformed the surface quartz and since the average SiO_2 on the surface is slightly greater than other intervals, the results manifest the growing energy of wind in recent years. Irrespective of superficial sediments, both SiO_2 and Zr are gradually growing with depth, displaying a negative correlation with metals. This suggests different sources of metals in the playa (Roy et al. 2006). Zr is a constructive element of heavy minerals such as zircon, ilmenite, and rutile. The surge in Zr shows that sediments were transported at a higher energy level in the past.

Hydrological characteristics

Geomorphologic elements provide key evidence to interpret geological and hydrological characteristics and environmental conditions. Three types of geomorphologic surfaces including salt crust, clay pan, and puffy ground, identified in the Sabzevar playa are construed as signs of hydrological characteristics of the playa as described below.

Salt crusts often appear at the latest stage of evaporation and/or are formed in a capillary zone where the evaporation rate is high (Rosen 1994). The general direction of groundwater flow in the Sabzevar basin is from east to west (Pourali 2020; Panahi et al. 2021) and there is a salt crust in the west. It is also worth noting that the topographical height declines toward the west. Thus, the groundwater level can be observed about 20 cm below the surface in the west. However, it cannot be less than 2 m from the surface due to the absence of water in incised channels located in the east and center of the playa (Pourali 2020). The evaporation rate depends on the groundwater level, with shallow levels increasing evaporation (Houston 2006). As a result, the western part has undergone more rapid evaporation. The groundwater of the Sabzevar plain in the sodium-chloride region of the piper diagram exhibits oversaturation in Na and Cl (Panahi et al. 2021). Thus, the groundwater chemistry and a higher rate of evaporation are evident in halite formation and the salt crust development of the west playa. The **puffy ground** represents the surface concentrated in the central Sabzevar playa. It is mostly formed at the surface when groundwater is subject to seasonal fluctuations with a high rate of evaporation. The evaporation leads to the shrinkage of the water level and expands the capacity of swelling in superficial sediments (Messing and Jarvis 1990; Elmore et al. 2008; Goudie 2018). Although the groundwater level was low in the summer at the time of the field study, this surface suggests that the water level had dropped locally and risen in different seasons. **Clay pan** represents the surface formed over the margin of the Sabzevar playa but is mostly extended to the east. It is often formed as a result of the low solubility of fine evaporite minerals such as carbonates and gypsum. It also shows the early stages of evaporation and the shallow level of water in the basin (Rahimpour-Bonab and Abdi 2012).

Conclusion

The Sabzevar playa documents the vertical heterogeneity of sediments at the surface to a depth of 1 m. Heterogeneity is caused by grain size, mineralogy, and sediment supply. Clastic minerals grow in abundance as the depth increases whereas evaporite minerals reflect an opposite trend. Quartz is the most prominent clastic mineral and its micro-morphology along boreholes reveals the mechanism of sediment transportation by the wind at the surface and by water in depth. A combination of mineralogical trends and groundwater chemistry suggests that brine contains ions such as Na–Ca–Mg–K–SO_4–Cl–CO_3. The geochemical processes led to evaporite minerals forming an evolved brine of Na–SO_4–Cl type. These findings prove that the concentration of authigenic clay minerals, including palygorskite, and sepiolite, increased at the surface sediments. Mineralogy and distribution of clay-sized minerals with geochemical analysis of oxides suggest a warm humid climate in the past, which has recently turned into a more arid one. Sedimentology and granulometry records illustrate greater fluctuations in the past with higher energy, implying that permanent rivers have probably flown through the Sabzevar basin as indicated by more pronounced chemical weathering at a depth of 1 m. The Sabzevar playa is classified as an unconventional bull's eye pattern with carbonates all around the margin, gypsum in the center, and halite in the west. The results suggest that the high groundwater level in the west was associated with marked evaporation and consequently the development of salt flats.

Supplementary Information The online version contains supplementary material available at https://doi.org/10.1007/s13146-022-00829-7.

Acknowledgements The authors would like to thank the vice president of the Ferdowsi University of Mashhad for the financial support of the project. We would like to express our great appreciation to Prof. Alireza Karimi for his help, valuable explanations and constructive suggestions during our study.

Author contributions All authors contributed to the study's conception and design. Material preparation, and data collection by MP. Data analysis was performed by MP, AS and ZH. MP wrote the first draft of the manuscript and all authors commented on previous versions of the manuscript. All authors read and approved the final manuscript.

Funding This work was funded by "The Ferdowsi University of Mashhad" (Grant no. 3-41832).

Availability of data and materials Most data generated or analyzed during this study are included in this published article and its supplementary information files. The rest data are available from the corresponding author on reasonable request.

Declarations

Conflict of interest The authors declare that they have no known conflict of financial interests or personal relationships that might have influenced the work reported in this paper.

References

Abdi L, Rahimpour-Bonab H, Mirmohammad-Makki M, Probst J, Langeroudi SR (2018) Sedimentology, mineralogy, and geochemistry of the Late Quaternary Meyghan Playa sediments, NE Arak, Iran: palaeoclimate implications. Arab J Geosci 11(19):1–18. https://doi.org/10.1007/s12517-018-3918-3

Argaman E, Singer A, Tsoar H (2006) Erodibility of some crust forming soils/sediments from the Southern Aral Sea Basin as determined in a wind tunnel. Earth Surf Process Landf J Br Geomorphol Res Group 31(1):47–63. https://doi.org/10.1002/esp.1230

Ashley GM (1978) Interpretation of polymodal sediments. J Geol 86(4):411–421. http://www.jstor.org/stable/30060027

Berberian M (1981) Active faulting and tectonics of Iran. Zagros Hindu Kush Himalaya. Geodyn Evol 3:33–69. https://doi.org/10.1029/GD003p0033

Blott SJ, Pye K (2001) GRADISTAT: a grain size distribution and statistics package for the analysis of unconsolidated sediments. Earth Surf Proc Land 26:1237–1248. https://doi.org/10.1002/esp.261

Chang H, An ZS, Wu F, Jin ZD, Liu WG, Song YG (2013) A Rb/Sr record of the weathering response to environmental changes in westerly winds across the Tarim Basin in the late Miocene to the early Pleistocene. Palaeogeogr Palaeoclimatol Palaeoecol 386(6):364–373. https://doi.org/10.1016/j.palaeo.2013.06.006

Czarnecki JB (1997) Geohydrology and evapotranspiration at Franklin Lake playa, Inyo 800 County, California. US Geological Survey Water-Supply Paper 2377:75

Deconinck JF, Amedro F, Baudin F, Godet A, Pellenard P, Robaszynski F, Zimmerlin I (2005) Late Cretaceous palaeoenvironments expressed by the clay mineralogy of Cenomanian–Campanian chalks from the east of the Paris Basin. Cretac Res 26(2):171–179. https://doi.org/10.1016/j.cretres.2004.10.002

Du S, Li B, Niu D, Zhang DD, Wen X, Chen D, Yang Y, Wang FN (2011) Age of the MGS5 segment of the Milanggouwan stratigraphical section and evolution of the desert environment on a kiloyear scale during the Last Interglacial in China's Salawusu River Valley: evidence from Rb and Sr contents and ratios. Chem Erde-Geochem 71:87–95. https://doi.org/10.1016/j.chemer.2010.07.002

Elmore AJ, Kaste JM, Okin GS, Fantle MS (2008) Groundwater influences on atmospheric dust generation in deserts. J Arid Environ 72(10):1753–1765. https://doi.org/10.1016/j.jaridenv.2008.05.008

Ercan HÜ, Karakaya MÇ, Bozdağ A, Karakaya N, Delikan A (2019) Origin and evolution of halite based on stable isotopes (δ37Cl, δ81Br, δ11B and δ7Li) and trace elements in Tuz Gölü Basin, Turkey. Appl Geochem 105:17–30. https://doi.org/10.1016/j.apgeochem.2019.04.008

Erfanian Kaseb H, Torshizian HA, Jahani D, Javanbakht M, Kohansal Ghadimvand N (2020) Effects of lithological and evolutionary processes on geochemical changes of Shahrokht-Yazdan Playa brines (east of Iran-west of Afghanistan). Arab J Geosci 13(20):1–17. https://doi.org/10.1007/s12517-020-05897-4

Eugster HP, Hardie LA (1978) Saline lakes. In: Lerman A (ed) Lakes. Springer, New York, pp 237–293

Farpoor MH, Khademi H, Eghbal MK (2002) Genesis and distribution of palygorskite and associated clay mineralsin Rafsanjan soils on different geomorphic surfaces. Iran Agricultural Research 21: 39–60

Farpoor MH, Neyestani M, Eghbal MK, Borujeni IE (2012) Soil–geomorphology relationships in Sirjan playa, south central Iran. Geomorphology 138(1):223–230. https://doi.org/10.1016/j.geomorph.2011.09.005

Folk RL, Ward WC (1957) The Brazos river bar. A study in the significance of grain size parameters. J Sediment Petrol 27:3–26. https://doi.org/10.1306/74D70646-2B21-11D7-8648000102C1865D

Friedman SP, Jones SB (2001) Measurement and approximate critical path analysis of the pore scale-induced anisotropy factor of an unsaturated porous medium. Water Resour Res 37:2929–2942. https://doi.org/10.1029/2000WR000095

Geological Survey of Iran (2005) Geological sheets of 7262 (Abbas-Abad), 7362 (Davarzan), 7462 (Bashtin), and 7562 (Sabzevar), Scale 1:100,000

Ghasemzadeh Ganjehie M, Karimi A, Zeinadini A, Khorassani R (2018) Relationship of soil properties with yield and morphological parameters of pistachio in geomorphic surfaces of Bajestan Playa, Northeastern Iran. J Agric Sci Technol 20(2):417–432

Goudie A (2018) Dust storms and ephemeral lakes. Desert 23(1):153–164. https://doi.org/10.22059/jdesert.2018.66370

Gustavson TC, Hovorka SD, Dutton AR (1994) Origin of satin spar veins in evaporite basins. J Sediment Res 64(1a):88–94. https://doi.org/10.1306/D4267D1B-2B26-11D7-8648000102C1865D

Hahnenberger M, Nicoll K (2014) Geomorphic and land cover identification of dust sources in the eastern Great Basin of Utah, USA. Geomorphology 204:657–672. https://doi.org/10.1016/j.geomorph.2013.09.013

Han L, Liu D, Cheng G, Zhang G, Wang L (2019) Spatial distribution and genesis of salt on the saline playa at Qehan Lake, Inner Mongolia, China. CATENA 177:22–30. https://doi.org/10.1016/j.catena.2019.01.040

Hardie LA, Smoot JP, Eugster HP (1978) Saline lakes and their deposits: a sedimentological approach. In: Matter A, Tucker ME (eds) Modern and ancient lake sediments 7–41. International Association of Sedimentologists, New York. https://doi.org/10.1002/9781444303698.ch2

Hminna A, Lagnaoui A, Zouheir T, Saber H, Schneider JW (2020) Late Triassic ichnoassemblage from a playa-lake system of the Coastal Meseta, Morocco: palaeoenvironmental and palaeoecological implications. J Afr Earth Sc 172:103995. https://doi.org/10.1016/j.jafrearsci.2020.103995

Hosseini Z, Gharechelou S, Nakhaei M, Gharechelou S (2016) Optimal design of BP algorithm by ACOR model for groundwater-level forecasting: a case study on Shabestar plain, Iran. Arab J Geosci 9(6):1–16. https://doi.org/10.1007/s12517-016-2454-2

Houston J (2006) Variability of precipitation in the Atacama Desert: its causes and hydrological impact. Int J Climatol J R Meteorol Soc 26(15):2181–2198. https://doi.org/10.1002/joc.1359

Ingebritsen SE, Sanford WE (1998) Groundwater in geologic processes. Cambridge University Press, Cambridge, New York, Melbourne. ISBN 0 521 49608 X. Geol Mag 136(6):697–711. https://doi.org/10.1017/S0016756899363329

Itamiya H, Sugita R and Sugai T (2019) Analysis of the surface microtextures and morphologies of beach quartz grains in Japan and implications for provenance research. Progress in Earth and Planetary Science 6(1):1–14. https://doi.org/10.1186/s40645-019-0287-9

Jackson ML (2005) Soil chemical analysis: advanced course. UW-Madison Libraries Parallel Press, Madison

Jalilian T, Taghian A, Lak R, Darvishi Khatooni J (2021) The Late Quaternary sedimentary sequences and environmental changes based on core studies in the Gavkhouni Playa (Central Iran). Environ Earth Sci 80(23):1–12. https://doi.org/10.1007/s12665-021-10040-x

Jones BF, Deocampo DM (2003) Geochemistry of saline lakes. Treatise on geochemistry 5:393–424. https://doi.org/10.1016/B0-08-043751-6/05083-0

Jouladeh Roudbar A, Eagderi S, Esmaeil HR (2015) Fishes of the Dasht-e Kavir basin of Iran: an updated checklist. Int J Aquat Biol 3(4):263–273. https://doi.org/10.22034/ijab.v3i4.105

Khormali F, Abtahi A (2003) Origin and distribution of clay minerals in calcareous arid and semi-arid soils ofFars Province, southern Iran. Clay Miner 38(4):511–527. https://doi.org/10.1180/0009855023740112

Krinsley DB and Geological Survey (U.S.) & Air Force Cambridge Research Laboratories (U.S.) (1970) A geomorphological and paleoclimatological study of the playas of Iran. Geological Survey, US Department of the Interior, Washington, DC

Li J, Qu X, Dong Z, Cai Y, Liu M, Ren X, Cui X (2021) Contribution of underlying terrain to sand dunes: evidence from the Qaidam Basin, Northwest China. J Arid Land 13(12):1215–1229. https://doi.org/10.1007/s40333-021-0028-y

Lukich V, Cowling S, Chazan M (2020) Palaeoenvironmental reconstruction of Kathu Pan, South Africa, based on sedimentological

data. Quat Sci Rev 230(3):106–153. https://doi.org/10.1016/j.quascirev.2019.106153
Martinez-Ruiz F, Kastner M, Gallego-Torres D et al (2015) Paleoclimate and paleoceanography over the past 20,000 yr in the Mediterranean Sea Basins as indicated by sediment elemental proxies. Quat Sci Rev 107:25–46. https://doi.org/10.1016/j.quascirev.2014.09.018
Mason B, Moore C (1982) Principles of geochemistry. Wiley, New York. https://doi.org/10.4236/jmp.2021.123015
May JH, Barrett A, Cohen TJ, Jones BG, Price D, Gliganic LA (2015) Late Quaternary evolution of a playa margin at Lake Frome, South Australia. J Arid Environ 122:93–108. https://doi.org/10.1016/j.jaridenv.2015.06.012
Messing I, Jarvis NJ (1990) Seasonal variation in field-saturated hydraulic conductivity in two swelling clay soils in Sweden. J Soil Sci 41(2):229–237
Mir RA, Jeelani GH (2015) Textural characteristics of sediments and weathering in the Jhelum River basin located in Kashmir Valley, western Himalaya. J Geol Soc India 86(4):445–458. https://doi.org/10.1007/s12594-015-0332-2
Neal JT (1972) Playa surface features as indicators of environment. In: Reeves CC (ed) Playa Lake symposium 967 Proceedings, ICASALS Publication 4. Texas Tech University, 968 Lubbock, TX, pp 107–132
Nelson DW, Sommers LE (1996) Total carbon, organic carbon, and organic matter. In Sparks DL, et al., Eds., Methods of Soil Analysis. Part 3, Chemical Methods, SSSA Book Series, No. 5, Soil Science Society of America, Madison, Wisconsin, USA, 961–1010
Owen LA, Bright J, Finkel RC, Jaiswal MK, Kaufman DS, Mahan S, Radtke U, Schneider JS, Sharp W, Singhvi AK, Warren CN (2007) Numerical dating of a Late Quaternary spit-shoreline complex at the northern end of Silver Lake playa, Mojave Desert, California: a comparison of the applicability of radiocarbon, luminescence, terrestrial cosmogenic nuclide, electron spin resonance, U-series and amino acid racemization methods. Quat Int 166(1):87–110. https://doi.org/10.1016/j.quaint.2007.01.001
Owliaie HR, Abtahi A, Heck RJ (2006) Pedogenesis and clay mineralogical investigation of soils formed on gypsiferous and calcareous materials, on a transect, southwestern Iran. Geoderma 134(1-2):62–81. https://doi.org/10.1016/j.geoderma.2005.08.015
Panahi G, Eskafi MH, Rahimi H, Faridhosseini A, Tang X (2021) Physical–chemical evaluation of groundwater quality in semi-arid areas: case study—Sabzevar plain, Iran. Sustain Water Resour Manag 7(6):1–15. https://doi.org/10.1007/s40899-021-00576-y
Pandarinath K, Prasad S, Gupta SK (1999) A 75 ka record of Palaeoclimatic changes inferred from crystallinity of illite from Nal Sarovar, western India. J Geol Soc India 54:515–522
Pardo A, Adatte T, Keller G, Oberhänsli H (1999) Paleoenvironmental changes across the Cretaceous-Tertiary boundary at Koshak, Kazakhstan, based on planktic foraminifera and clay mineralogy. Palaeogeogr Palaeoclimatol Palaeoecol 154(3):247–273. https://doi.org/10.1016/S0031-0182(99)00114-5
Pettit D, Fontana P (2019) Comparison of sodium chloride hopper cubes grown under microgravity and terrestrial conditions. Npj Microgravity 5(1):1–7. https://doi.org/10.1038/s41526-019-0085-0
Pourali M, Sepehr A, Mahmudy Gharaie MH (2020) Depositional pattern of sediments in a dry-lake Playa in NE Iran; Implication for geomorphologic characteristics. Desert Ecosyst Eng J 3(1):11–24
Pourali M (2020) A study of late Quaternary geomorphology evolution at Sabzevar playa using depositional records and mineral composition. Ph.D. thesis of Geomorphology, Ferdowsi University of Mashhad
Rahimpour-Bonab H, Abdi L (2012) Sedimentology and origin of Meyghan lake/playa deposits in Sanandaj-Sirjan zone, Iran. Carbonates Evaporites 27(3):375–393. https://doi.org/10.1007/s13146-012-0119-0
Rayment GE, Lyons DJ (2011) Soil chemical methods: Australasia, vol 3. CSIRO Publishing, Clayton
Richoz S, Baldermann A, Frauwallner A et al (2017) Geochemistry and mineralogy of the Oligo-Miocene sediments of the Valley of Lakes, Mongolia. Palaeobiodivers Palaeoenviron 97(1):233–258. https://doi.org/10.1007/s12549-016-0268-6
Rosen MR (1994) The importance of groundwater in playas: a review of playa classifications and the sedimentology and hydrology of playas. Geol Soc Am 289:1–18. https://doi.org/10.1130/SPE289-p1
Roy PD, Smykatz-Kloss W, Sinha R (2006) Late Holocene geochemical history inferred from Sambhar and Didwana playa sediments, Thar Desert, India: comparison and synthesis. Quat Int 144(1):84–98. https://doi.org/10.1016/j.quaint.2005.05.018
Roy PD, Caballero M, Lozano R, Smykatz-Kloss W (2008) Geochemistry of late quaternary sediments from Tecocomulco Lake, central Mexico: implication to chemical weathering and provenance. Geochemistry 68:383–393. https://doi.org/10.1016/j.chemer.2008.04.001
Ruffell A, McKinley JM, Worden RH (2002) Comparison of clay mineral stratigraphy to other proxy palaeoclimate indicators in the Mesozoic of NW Europe. Philos Trans R Soc Lond Ser A Math Phys Eng Sci 360(1793):675–693. https://doi.org/10.1098/rsta.2001.0961
Schroder T, van't Hoff J, Lopez-Saez JA, Viehberg F, Melles M, Reicherter K (2018) Holocene climatic and environmental evolution on the southwestern Iberian Peninsula: a high-resolution multi-proxy study from Lake Medina (Cádiz, SW Spain). Quat Sci Rev 198:208–225. https://doi.org/10.1016/j.quascirev.2018.08.030
Shang Y, Last WM (1999) Mineralogy, lithostratigraphy and inferred geochemical history of North Ingebrigt Lake, Saskatchewan. Bull Geol Surv Canada 10:95–110. https://doi.org/10.4095/211112
Sharifi Paichoon M (2021) Tectonic geomorphology and Quaternary evolution of playas: a case study of Ernan Playa, central Iran. Arab J Geosci 14(13):1–18. https://doi.org/10.1007/s12517-021-07631-0
Sinha R, Smykatz-Kloss W, Stüben D, Harrison SP, Berner Z, Kramar U (2006) Late Quaternary palaeoclimatic reconstruction from the lacustrine sediments of the Sambhar playa core, Thar Desert margin, India. Palaeogeogr Palaeoclimatol Palaeoecol 233(3–4):252–270. https://doi.org/10.1016/j.palaeo.2005.09.012
Smoot JP, Lowenstein TK (1991) Depositional environments of nonmarine evaporites. Dev Sedimentol 50:189–347. https://doi.org/10.1016/S0070-4571(08)70261-9
Smykatz-Kloss W, Roy PD (2010) Evaporite mineralogy and major element geochemistry as tools for palaeoclimatic investigations in arid regions: a synthesis. Bol Soc Geol Mex 62(3):379–390. https://doi.org/10.18268/BSGM2010v62n3a5
Solotchina EP, Sklyarov EV, Solotchin PA et al (2012) Reconstruction of the Holocene climate based on a carbonate sedimentary record from shallow saline Lake Verkhnee Beloe (western Transbaikalia). Russ Geol Geophys 53(12):1351–1365. https://doi.org/10.1016/j.rgg.2012.10.008
Środoń J (1984) X-ray powder diffraction identification of illitic materials. Clay Clay Miner 32(5):337–349. https://doi.org/10.1346/CCMN.1984.0320501
Stankevica K, Klavins M, Vincevica-Gaile Z, Kalnina L, Kaup E (2020) Accumulation of metals and changes in composition of freshwater lake organic sediments during the Holocene. Chem Geol 539:119502. https://doi.org/10.1016/j.chemgeo.2020.119502
Torshizian H (2009) rains evolution and evaporate minerals formation in Saghand playa in central Iran, and compare with some saline lake in the world. Iran J Crystallogr Mineral 17(1):43–54

Tucker ME (ed) (2001) Sedimentary petrology: an introduction to the origin of sedimentary rocks, 3rd edn. Wiley, New York

Vaezi A, Ghazban F, Tavakoli V, Routh J, Beni AN, Bianchi TS, Curtis JH, Kylin H (2019) A late Pleistocene-Holocene multi-proxy record of climate variability in the Jazmurian playa, southeastern Iran. Palaeogeogr Palaeoclimatol Palaeoecol 514:754–767. https://doi.org/10.1016/j.palaeo.2018.09.026

Vos K, Vandenberghe N and Elsen J (2014) Surface textural analysis of quartz grains by scanning electronmicroscopy (SEM): From sample preparation to environmental interpretation. Earth-Science Reviews 128:93–104. https://doi.org/10.1016/j.earscirev.2013.10.013

van de Wiel HJ (2003) Determination of elements by ICP-AES and ICP-MS. National Institute of Public Health and the Environment (RIVM), Bilthoven, pp 1–19

Warren JK (2006) Evaporites: sediments, resources and hydrocarbons. Springer Science & Business Media, Berlin

Xia Z, Lin Y, Wei H, Hu Z, Liu C, Li W (2022) Reconstruct hydrological history of terrestrial saline lakes using Mg isotopes in halite: a case study of the Quaternary Dalangtan playa in Qaidam Basin, NW China. Palaeogeogr Palaeoclimatol Palaeoecol 587:110804. https://doi.org/10.1016/j.palaeo.2021.110804

Xie Q, Chen T, Zhou H, Xu X, Xu H, Ji J, Lu H, Balsam W (2013) Mechanism of palygorskite formation in the Red Clay Formation on the Chinese Loess Plateau, northwest China. Geoderma 192:39–49. https://doi.org/10.1016/j.geoderma.2012.07.021

Yan JP, Hinderer M, Einsele G (2002) Geochemical evolution of closed-basin lakes: general model and applicationto Lakes Qinghai and Turkana. Sedimentary Geology 148(1-2): 105-122. https://doi.org/10.1016/S0037-0738(01)00212-3

Yechieli Y, Wood WW (2002) Hydrogeologic processes in saline systems: playas, sabkhas and saline lakes. Earth Sci Rev 58(3–4):343–365. https://doi.org/10.1016/S0012-8252(02)00067-3

Zandifar S, Tavakoli V, Vaezi A, Naeimi M, Naderi Beni A, Sharifi-Yazdi M, Routh J (2022) Influence of transport mechanism on playa sequences, late Pleistocene–Holocene period in Jazmurian Playa, southeast Iran. Arab J Geosci 15(7):1–13. https://doi.org/10.1007/s12517-022-09918-2

Zhang M, Liu X, Yu Z, Wang Y (2022) Paleolake evolution in response to climate change since middle MIS 3 inferred from Jilantai Salt Lake in the marginal regions of the ASM domain. Quat Int 607:48–57. https://doi.org/10.1016/j.quaint.2021.06.017